Available online at www.sciencedirect.com
SCIENCE DIRECT
Journal of Power Sources 150 (2005) 78–85
JOURNAL OF POWER SOURCES
www.elsevier.com/locate/jpowsour

New design of a PEM fuel cell air automatic climate control unit

R. Glises *, D. Hissel, F. Harel, M.C. Péra

L2ES (Electrical Engineering and Systems Laboratory), UFC-UTBM Joint Research Unit EA-3898, UTBM, Bâtiment F, 90010 Belfort Cedex, France

Received 1 June 2004; received in revised form 6 February 2005; accepted 7 February 2005
Available online 26 April 2005

Abstract

Temperature and hydration management are very important points for operating fuel cell systems and for optimizing their energy balance. In this paper, the design and the manufacture of an air conditioning device dedicated to proton exchange membrane (PEM) fuel cells are presented. Experimental thermal behavior laws are described and are intended to be integrated in a fuel cell powertrain model to drive the fuel cell without using an expensive and not adapted hygrometry measurement system. Experiments on a low power-testing bench (500 W) have been carried out, showing the efficiency of the system. Fuel cell polarization curves are shown, overheating and thermal inertia durations are also provided and taken into account for optimizing the regulation.

Keywords: Fuel cell system modelling; Hydration management; Air conditioning device

1. Introduction

Hydration content of the fuel cell membrane is a key point to get a good efficiency [1,2] of a PEM fuel cell stack. The produced water during electrochemical reaction at the cathode side is not usually sufficient to guarantee good moisture content, in the whole range of operating current density and temperature. Additional water has to be brought to the system by hydrogen, air or both [3]. The water balance is not easy to reach as too much water leads to a flood of the electrodes and not enough water will dry the membrane [4]. The behavior of the stack versus this phenomenon depends on a great amount of parameters: type and thickness of the membrane, catalyst layer, electrode backing and flow channels, temperatures of the different parts of the stack. Furthermore, the amount of water dragged by the gas depends on the humidity rate of the gas and on its temperature. Moreover, mastering the gas temperature and its humidity rate costs a lot of energy and lowers the global efficiency of the fuel cell system. In order to study this critical issue, an air conditioning system has been designed and realized for a low power PEM fuel cell test bench (500 W). After having described different hydration systems and justified our choice, the second part of this paper describes the testing bench [5,6] and the principle of the air conditioning system. The choice of the boiler for this application is valid for obtaining a reliable, dynamic and low cost hydration management system, moreover easy to control. It has been built and adapted to the low power of the PEMFC. The following part of the paper shows experimental results to demonstrate the ability of the system to ensure both a given humidity rate and a given temperature of the input air. The thermal inertia of the boiler and the heater are also shown. The last part describes thermal behavior experimental laws of the air conditioning system. The thermal characterization laws are obtained, thanks to experimental temperatures and time durations of the air conditioning ancillaries transient states. Theoretical laws permitting to have enthalpies as function of air pressure are also calculated. Law association is then integrated in an open loop control of the air conditioning device. It finally permits to control the air temperature and hygrometry levels without using a very precise (and also very expensive) optical hygrometer that cannot be considered for PEM fuel cell embedded applications.

* Corresponding author. Tel.: +33 384 583 600; fax: +33 384 583 636.
E-mail address: raynal.glises@univ-fcomte.fr (R. Glises).

0378-7753/$ – see front matter © 2005 Elsevier B.V. All rights reserved.
doi:10.1016/j.jpowsour.2005.02.019

Nomenclature

A, B, C, D	constant coefficient (no dimension)
c_p	specific heat ($J\,kg^{-1}\,K^{-1}$)
C_p	heat capacity ($J\,K^{-1}$)
h	specific enthalpy ($J\,kg_{as}^{-1}$)
h_{in}	input air specific enthalpy ($J\,kg_{as}^{-1}$)
h_{out}	output air specific enthalpy ($J\,kg_{as}^{-1}$)
h_r	saturated air specific enthalpy ($J\,kg_{as}^{-1}$)
p_t	absolute pressure (Pa)
p_{vs}	saturated air absolute pressure (Pa)
P_{ext}	external heat losses (W)
P_r	feeding power (steady state) (W)
$P_{r'}$	feeding power (transient state) (W)
$P_{th1\text{-}2}$	thermal power transmitted to the air (W)
q_m	mass flow ($g\,l^{-1}$)
q_v	volume flow rate ($N\,l\,min^{-1}$)
Q	amount of heat (J)
T	dry air temperature (°C)
T_{ext}	room temperature (°C)
$T_{air\ input}$, T_{in}	input temperature of the air (°C)
$T_{air\ output}$, T_{out}	output temperature of the air (°C)
T_r	saturated air temperature (°C)

Greek symbols

Δt	time duration (s)
ρ	density ($kg\,m^{-3}$)
χ	moisture content ($kg_{H_2O}\,kg_{as}^{-1}$)

2. Different kinds of hydration management systems

This section is devoted to a short state of existing hydration systems already available for PEM fuel cells.

2.1. Water injection

Heated water is injected in a column where air circulates. A controlled airflow enters at the bottom of the column while a controlled water stream is injected at the top. As the air rises, it gets wet [7]. Vapour exchange is favoured by metallic rolls inside the column. The water quantity to be injected is computed versus the air temperature, pressure, flow and the required humidity rate. A bleeder located at the column bottom collects water, which has not been transferred to the air. Water is heated before entering the system by an evaporator and its temperature is one of the parameters to be controlled. However, the exchange efficiency is less than 1 as liquid water in the bleeder witnesses. As this amount of liquid water is difficult to evaluate accurately, there is a discrepancy between the actual humidity rate and the humidity set point.

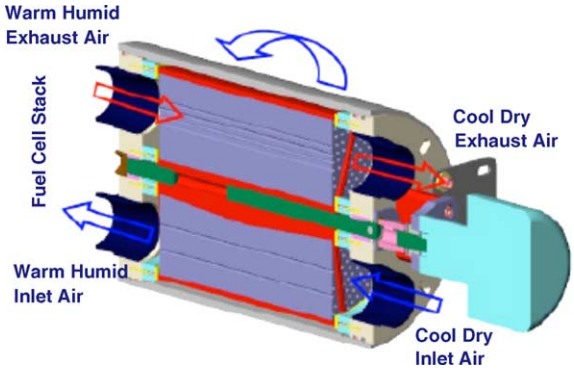

Fig. 1. Enthalpy wheel humidifier [8].

2.2. Enthalpy wheel humidifier

This device shown in Fig. 1 reuses the enthalpy of the outlet gas to humidify and warm the inlet fresh air. It consists in a porous cylindrical wheel, coated with desiccant, rotating slowly inside the housing. Warm, humid exhaust air from the fuel cell enters the humidifier. The rotating drum absorbs the exhaust water vapour transferring it to the cool dry inlet stream. Other exhaust gases continue, thanks to the drum desiccant coating. This device simplifies greatly the system, it avoids the output condenser, and it saves energy as it recovers exhaust enthalpy. However, it is hard to control accurately the humidity and the temperature of the inlet air. It depends on the temperature and humidity of the exhaust air, i.e. on the stack operating point. It might also introduce instabilities in the system control. This attractive solution can be useful in an operating system, as long as the fuel cell stack has been deeply characterized versus the air parameters and the humidifier performances are well known. It should be firstly studied and compared with a laboratory device, which allows repeatable air conditioning, independent from the stack loading.

2.3. Boiler

This device consists in the injection of an external air in the bottom of a bottle filled with water. It is the system that is used in the first stage of the proposed air climate control unit. The required temperature of the water and finally of the air obtained at the output of the boiler is ensured, thanks to thermal resistances. The required output air hygrometry of such ancillaries leads to 100%, whereas a following heater allows obtaining different values of air temperature and hygrometry at the entrance of the stack. The initial choice of the device is accounted for obtaining a reliable, faithful and not expensive hydration system allowing minimizing the thermal transient duration. This point is a very important one considering future dynamic applications. It also permits to work in a very large temperature and hygrometry band and to have a stable regulation loop.

3. Testing bench description

3.1. The stack

The stack under test has been supplied by ZSW Germany. It is composed of 20 cells. The active area is 100 cm^2. It is fed on the anode side with dry, pure hydrogen. It can be fed on the cathode side either with pure oxygen or air, dry or humid. The operating temperatures take range from 20 to 70 °C. The relative gas pressure has to be kept under 0.5 bar and the pressure drop between anode and cathode must remain under 250 mbar. The cooling water, circulating in the bipolar plates must be deionized (electrical conductivity <2 $\mu S\,cm^{-1}$). The maximal electrical power output is 600 W under 12 V [9].

3.2. The air conditioning design

This paper highlights the design of the air circuit for the control of both its temperature and humidity rate. The operating range of the air conditioning is bounded by two equal humidity rate curves: $\chi_1 = 0.015\,kg_{vap}\,kg_{gas}^{-1}$ and $\chi_2 = 0.15\,kg_{vap}\,kg_{gas}^{-1}$.

Fig. 2 shows the air conditioning circuit principle. It is made of four elements:

- the boiler saturates air at the chosen due point temperature;
- the condenser cools the saturated air to reach the desired amount of water;
- the separator evacuates the condensed water;
- the heater warms the gas to the required temperature and due point.

The airflow is determined according to the load current and controlled through a mass flow regulator. The due temperature is calculated according to the required temperature and hygrometry, and the corresponding absolute pressure. Dry (or not) incoming air goes firstly through the boiler. At the boiler output, air presents a 100% hygrometry level and a temperature T_r. A discrepancy between the due temperature T_r and the dry temperature set point T implies the warming of the boiler. Then, wet air is cooled in the condenser to extract the required amount of water from the air (in order to obtain the required air hygrometry level at the stack input). The separator ensures the evacuation of the condensed water.

Finally, the temperature is also measured at the stack input (Fig. 2). In the case of a difference between the measured temperature and the required input gas temperature, the heater can be switched on.

In order to check the reliability and faithfulness of the air management device, an optical hygrometer has been

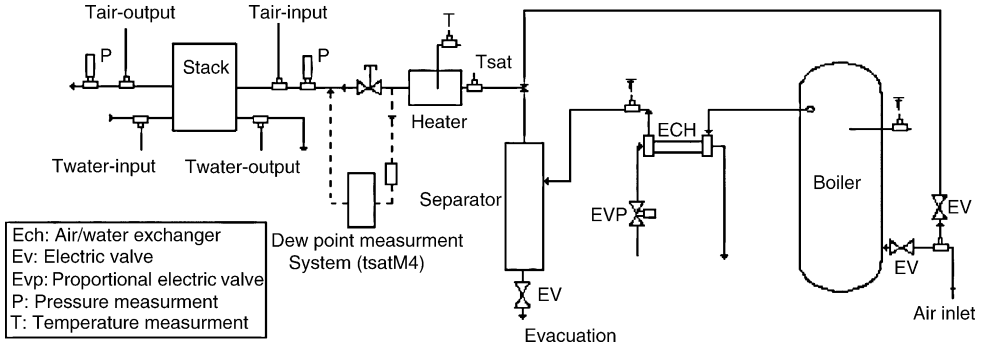

Fig. 2. Air conditioning system.

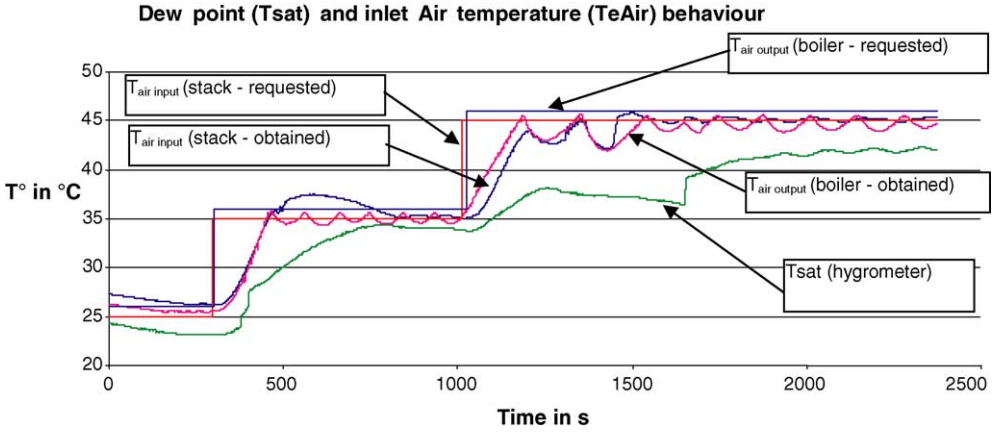

Fig. 3. Testing bench temperature responses.

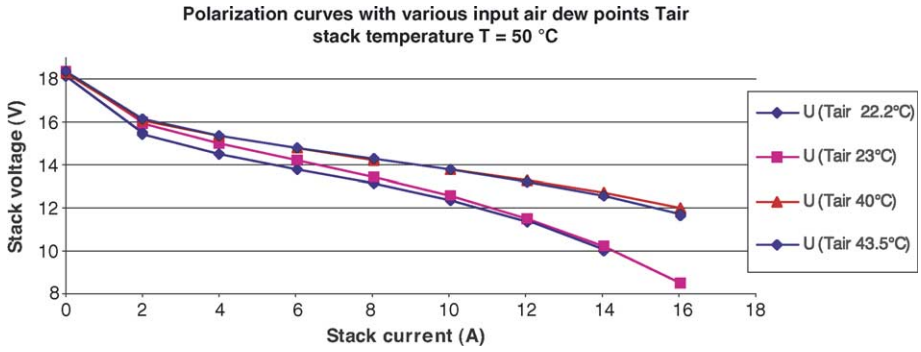

Fig. 4. Polarization curves measured under different dew points of the input air.

temporarily placed at the stack input. However, it is not finally involved in the process regulation because of its low time dynamic response (shown in Fig. 3) and its high price. The whole hygrometry setting system is also operating in a so-called open loop mode.

4. Experimental results

The air conditioning device allows investigating the influence of the temperature of the input air and its humidity on the stack behaviour. The aim of this type of study is to determine optimized operating conditions for the whole fuel cell system. The obtained temperatures and hygrometry inertia and reliability are also shown in this sectionmpared to the required ones.

4.1. Temperatures reliability for a 100% required humidity rate

A test has been realized for determining temperature reliability for a 100% humidity rate at the stack air input. Three operating points at the dew point are required:

$T_r = 25\,^{\circ}\mathrm{C}, \quad T_{\text{air-input}} = 26\,^{\circ}\mathrm{C}/T_r = 35\,^{\circ}\mathrm{C},$

$T_{\text{air-input}} = 36\,^{\circ}\mathrm{C}/T_r = 45\,^{\circ}C, \quad T_{\text{air-input}} = 46\,^{\circ}\mathrm{C}$

Fuel cell power generation is 490 W and stoichiometry factors at the anode and the cathode are, respectively, 2 and 4. Hydrogen volume flows at the input and output of the anode are, respectively, 9.86 and 4.78 N l min^{-1}. At the cathode, air volume flows are in the same order: 46.86 and 43.43 N l min^{-1}.

Fig. 3 gives temperature responses as function of time *t*. A relative reliability between requested and obtained temperatures can be seen. Two degreescelsius temperature differences can nevertheless be seen between output required temperature and output obtained temperature at the boiler. This difference is probably bounded by thermal heat losses of the boiler. Moreover, the final hygrometry rate measured by the optical hygrometer is 97% showing the well behaviour of the proposed air conditioning system. Problem of T_{sat} given by the hygrometer is the high thermal inertia of this device compared to required parameters. Moreover, such apparatus depends on local thermal and fluidic phenomenon. Inertia and fall of indicate temperature between 1200 and 1700 s are bounded by local condensation drop.

Generally, temperature differences between required and obtained temperatures come from the thermal heat losses, particularly at the boiler and the heater. To minimize these differences, it is also necessary to quantify very precisely all these losses at different operating levels. A good characterization of these points also permits to regulate the air management device faithfully.

Fig. 4 shows experimental polarization curves for a 100% humidity rate. They represent the stack voltage as functions of the current for different due points temperatures for the input air taking range from 22.2 to 43.5 °C. The stack temperature is kept constant (at 50 °C). The stack output cooling water temperature has been considered as representative of this stack internal temperature. The air enters the stack at its dew point, which varies between the different curves. The influence of this parameter on the stack response is here clearly demonstrated, as the available electrical power is increasing with the inlet air dew point.

4.2. Polarization characteristics—validation of the device

Fig. 5 shows a polarization curve, supplying the stack with unsaturated air (T_{stack} = 50 °C, $T_{air\ input}$ = 30 °C and hygrometry rates are 50% and 75%). Software developed with Labview permits to drive the boiler, heat exchanger and final heater in order to obtain the requested input fluid parameters for the stack. The software is validated thanks to the responses of the temperature and hygrometer sensors located at the input of the stack.

5. Thermal characterization of the experimental air circuit

The proposed experimental characterizations also permit to define with a very good accuracy the thermophysical characteristics of the thermal losses of the boiler and the heater.

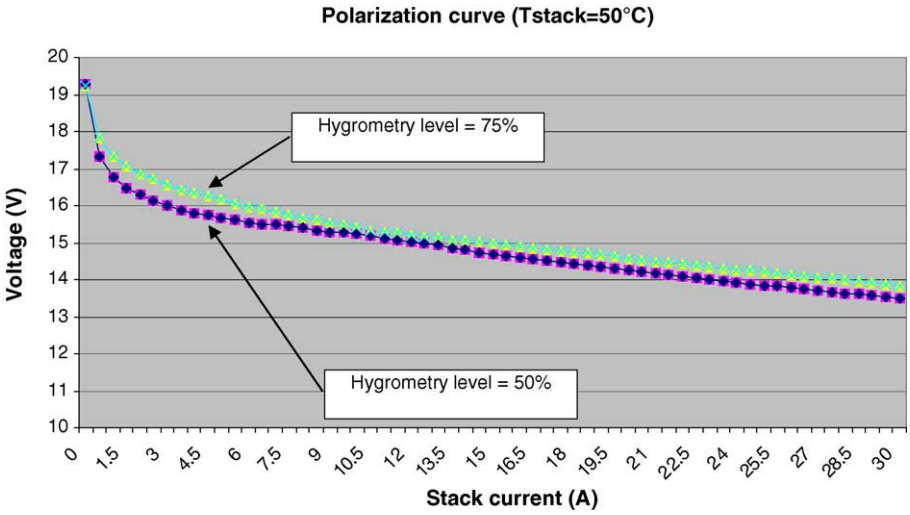

Fig. 5. Stack polarization curves with air at 50% and 75% humidity rates ($T_{\text{air input}} = 30\,^{\circ}\text{C}$).

Such identification also permits to define precisely the behaviour laws of the air conditioning system. Theoretical laws of the air behaviour [10] have permitted to obtain real thermal powers to bring to the boiler and to the heater to have the required air humidity and temperature at the input of the fuel cell for different fluid molar flows and absolute pressures taking range from 1 to 4 bar. Then, experimental thermal losses of the boiler and the heater are expressed as functions of the input and output temperatures of both apparatus for different fluid molar flows. The sum of theoretical power and experimental thermal losses of apparatus also allows evaluating electrical power sources at the boiler and the heater as function of the required humidity and temperature at the input of the fuel cell.

5.1. Air enthalpy as a function of temperature and absolute pressure

The feeding of the stack is made with atmospheric pressure air. The enthalpy h_r of the saturated air has to be calculated as a function of the temperature T and of the absolute pressure p_t. An approximated expression of the pressure of the saturated air is defined by the parabolic equation (1), valid between 10 and 70 °C.

$$p_{vs} = 9.35T_r^2 - 326T_r + 5432 \tag{1}$$

Enthalpy h_r is given by equation (2) where χ is the humidity ratio and T_r is the saturation temperature. This expression is given for 1 kg of dry air.

$$h_r = T_r + \chi(2490 + 1.96T_r) \tag{2}$$

The humidity ratio is calculated according to:

$$\chi = \frac{0.622p_{vs}}{p_t - p_{vs}} \tag{3}$$

Equations (1) and (3) in equation (2) allow obtaining a new expression of enthalpy given by equation (4):

$$h_r = \frac{2.057T_r^3 + 14402T_r^2 + (p_t - 503452)T_r + 8408736}{p_t - (9.35T_r^2 - 326T_r + 5432)} \tag{4}$$

The evolutions of enthalpy in a 50–600 kJ kg^{-1} range are the considered functions of the saturation temperature for absolute pressures from 10^5 to 4×10^5 Pa.

A second-order polynomial equation of the enthalpy as function of the saturation temperature at the considered absolute pressures can be easily obtained (5).

$$h_r = AT_r^2 - BT_r + C \tag{5}$$

Values of constants *A*–*C* are given in Table 1. They also depend on absolute air temperature in the air channel.

5.2. Thermal characterization of the boiler and heater without external heat losses

5.2.1. Power supply at the boiler

Case of a thermal steady state and an absolute air pressure of 10^5 Pa, the theoretical power of the system without heat losses is expressed through the balance of the enthalpies on the entrance and output fluid channels (equation (6)).

$$P_{th1} = \rho q_v(h_{out} - h_{in}) \tag{6}$$

Table 1
Polynomial constants *A*–*C* for different absolute air pressures

Absolute pressure p_t (Pa)	A (kJ kg^{-1} °C^{-2})	B (kJ kg^{-1} °C^{-1})	C (kJ kg^{-1})
1×10^5	0.230	8.43	133.3
2×10^5	0.148	8.09	171.1
3×10^5	0.085	3.78	92.24
4×10^5	0.067	3.34	92.42

In that expression, enthalpies are calculated with equation (4). The theoretical power of the boiler can be expressed as a function of the entrance fluid hygrometry rate φ for different values of the required air temperatures T (25–55 °C). The absolute pressure p_t is 10^5 Pa, whereas the heat flow is about $q_v = 15\,\mathrm{N\,l\,min^{-1}}$ and $T_{in} = 20\,^\circ\mathrm{C}$. Software then allows to express the power supply P_{th1} as a function of the hygrometry rate at the atmospheric pressure p_t. It can be expressed thanks to equation (7):

$$P_{th1} = A(T)\varphi + B(T) \tag{7}$$

Expressions of $A(T)$ and $B(T)$ can be easily literally determined after having drawn their evolution. Then, approximation laws of parameters A and B expressed in equation (7) give the final expression (8) of the supply power P_{th1} as function of required φ and T:

$$P_{th1} = (0.0744T^2 - 3.4218T + 54.397)\varphi - 0.0006T^3 + 0.0611T^2 - 1.7449T + 16.373 \tag{8}$$

For a complete characterization of the system in the operating range, it is necessary to consider different airflow alimentations. Indeed, different stoichiometry factors can be required imposing also variable airflows. Tests are realized for different mass airflows available from a minimum value to $1.6\,\mathrm{g\,s^{-1}}$. Obtained approximation laws are given in equation (9):

$$\frac{P_{th1}}{q_m} = (0.2978T^2 - 13.701T + 217.82)\varphi - 0.0458T^2 + 4.1286T - 69.416 \tag{9}$$

All these laws have been defined considering operating air conditions at $T_{in} = 20\,^\circ\mathrm{C}$ for different airflows feeding. The temperature is the room temperature. Nevertheless, future tests taking into account variable external conditions will be carried out for higher PEMFC powers thanks to a climate chamber.

5.2.2. Power supply to the heater

In the same way as the boiler, the expression of the supply power for the heater is given by expression (10):

$$P_{th2} = (0.0225T^2 - 1.2604T + 14.204)\varphi^2 + (-0.0156T^2 + 0.3033T + 4.947)\varphi - 0.0025T^2 + 0.6242T - 13.128 \tag{10}$$

and for different mass air flows, it becomes for input conditions at $p_t = 10^5$ Pa (11):

$$\frac{P_{th2}}{q_m} = (0.0901T^2 - 5.0413T + 56.813)\varphi^2 + (-0.0624T^2 + 1.2133T - 19.789)\varphi - 0.0064T^2 + 2.1943T - 46.987 \tag{11}$$

In expression (11), φ and T are, respectively, the required hygrometry and temperature at the air input of the stack.

5.3. Thermal characterization of the boiler and heater external heat losses

Considering the exhaustive heat power generation at the boiler and the heater, taking into account conduction, convection and radiation heat losses, only an experimental study allows to obtain the real thermal losses for the steady-state thermal heat transfer. Obtained values of the external heat losses are to be added to theoretical power supplies for each element to calculate final efficiency of the complete system. It can be expressed thanks to equation (12):

$$P_{ext} = P_r - P_{th} \tag{12}$$

with P_r the power actually supplied to the element, to ensure output thermodynamic constraints.

Experimental tests permit to obtain an approximation law of P_{ext} for different required hygrometries, output air temperatures and mass airflows. The obtained laws are linear and given by equations (13) and (14):

$$P_{ext1} = 2.32(T_{air\,output} - T_{ext}) \tag{13}$$

$$P_{ext2} = 0.1725(T_{air\,output} - T_{ext}) \tag{14}$$

5.4. Determination of the specific energy per degree of the boiler and the heater

Dynamic tests showing thermal transient states of these elements allow obtaining the specific energy per degree. Its value translates the duration of the transient thermal transfer between power generated and loose in the boiler and the heater. Finally, it gives an indication about the dynamic thermal response of the air circuit.

The expression of the energy variation of the considered system is estimated with a transient experimental test, supplying the element with the power $P_{r'}$ during a temperature increasing time Δt. It is given thanks to equation (15):

$$C_p(T_{out} - T_{ext}) = [P_r - (\rho q_v(h_{air\,m} - h_{in}) + P_{ext})]\Delta t \tag{15}$$

Parameter $h_{air\,m}$ represents the specific enthalpy of the air calculated to the arithmetic average temperature $(T_{out} + T_{in})/2$. It is then possible to obtain the specific energy per degree C_p of the boiler. Fig. 6 shows the evolution of the air output temperature during the transient thermal phase. Characteristics of that test are: $T_{air\,ouput} = 61\,^\circ\mathrm{C}$, $T_{air\,input} = 24.2\,^\circ\mathrm{C}$, $h_{rm} = 189.24\,\mathrm{kJ\,kg_{as}^{-1}}$, $h_{in} = 24.2\,\mathrm{J\,kg_{as}^{-1}}$, $q_v = 0.017\,\mathrm{l\,s^{-1}}$. The estimated duration of the thermal transient phase is $\Delta t = 1104$ s. Calculated C_p for the boiler is about $28{,}600\,\mathrm{J\,K^{-1}}$. Different tests have shown a thermal transient duration constant with t in our operating range.

As shown in Fig. 7, test characteristics for the determination of the specific heat of the heater are the following ones:

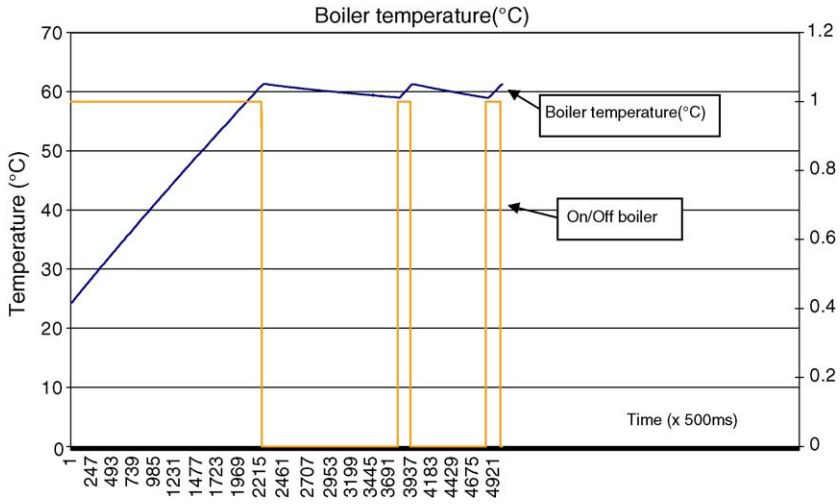

Fig. 6. Temperature evolution of the boiler ($T_{\text{air output}} = 60\,^{\circ}\text{C}$).

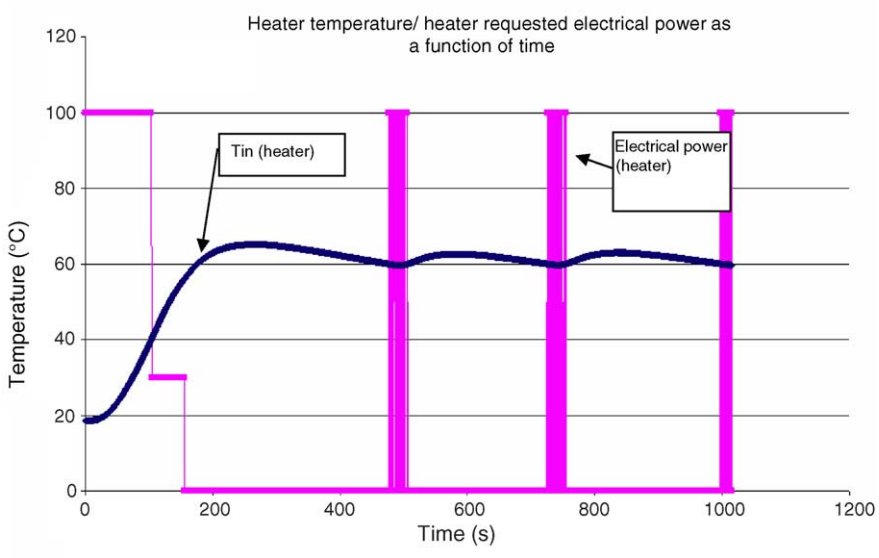

Fig. 7. Temperature evolution of the heater ($T_{\text{air output}} = 60\,^{\circ}\text{C}$).

$T_{\text{air output}} = 65\,^{\circ}\text{C}$, $T_{\text{ext}} = 22\,^{\circ}\text{C}$, heat generation $Q = 12\,\text{kJ}$ and the initial temperature $T_{\text{in}} = 18.6\,^{\circ}\text{C}$. The estimated duration of the thermal transient phase is $\Delta t = 1104\,\text{s}$. Calculated C_{p} for the heater is about $236\,\text{J K}^{-1}$.

6. Conclusion

Water management in a PEM fuel cell stack is a critical point. Therefore, the conditioning of the input air must be controlled. The designed device, which has been presented and realized in this study, allows controlling both the temperature and the humidity rate of a PEM fuel cell incoming air. The influence of these parameters on the stack performances can thus be easily investigated on a PEM testing bench [11]. The results allow defining the best operating conditions for the stack. Moreover, a balance of the auxiliaries consumptions will lead to the evaluation of the output net power of the fuel cell generator.

A model of the subsystems' behaviour laws has been elaborated. It allows determining the temperature references to reach the required characteristics for the fuel cell incoming air, taking into account thermal losses of the boiler and the heater. It also allows using the hydration system without a very expensive optical hygrometer having a too important measurement time response. It is then necessary to define functioning laws of the air circuit, the boiler and the heater for different mass flows, air temperatures and hygrometry rates. This model is also integrated in the open loop control of the air feeding. The described methodology applied to a

specific kind of fuel cell is a general methodology to simplify in a near future higher power fuel cell hydration systems. Only the constants of equations in this paper will have to be adapted to higher power stacks.

References

[1] J.J. Baschuk, L. Xianguo, Modelling of polymer membrane fuel cells with variable degrees of water flooding, J. Power Sources 86 (2000) 181–196.
[2] D.R. Sena, E.A. Ticianelli, V.A. Paganin, E.R. Gonzalez, Effect of water transport in a PEFC at low temperatures operating with dry hydrogen, J. Electroanal. Chem. 477 (1999) 164–170.
[3] T. Van Nguyen, M.W. Knobbe, A liquid water management strategy for PEM fuel cell stacks, J. Power Sources 114 (2003) 70–79.
[4] T. Okada, G. Xie, Y. Tanabe, Theory of management at the anode side of polymer electrolyte fuel cell membranes, J. Electroanal. Chem. 413 (1996) 49–65.
[5] F. Harel, S. Jemeï, X. François, M.C. Péra, D. Hissel, J.M. Kauffmann, Experimental investigations on PEMFC: a test bench design, in: Proceedings of the FDFC'02 Conference, Forbach, France, 2002, pp. 65–72.
[6] X. François, M.C. Péra, D. Hissel, J.M. Kauffmann, Design of a test bench for a low power PEMFC, in: Proceedings of the EPEFCF'01 Conference, Lucerne, Switzerland, 2001, pp. 491–499.
[7] http://www.serv'instrumentation.fr/.
[8] http://www.humidicore.com.
[9] S. Jemeï, D. Hissel, M.C. Péra, J.M. Kauffmann, On-board fuel cell power supply modeling thanks to neural network methodology, J. Power Sources 124 (2) (2003) 479–486.
[10] Rohsenow, Hartnett, Handbook of Heat Transfer, Mcgraw-Hill.
[11] D. Hissel, M.C. Péra, J.M. Kauffmann, Automotive fuel cell power generators diagnosis, J. Power Sources 128 (2) (2004) 239–246.